

## Frequency-Time Domain Analysis of Electrochemical Noise of Passivated AM350 Stainless Steel for Aeronautical Applications

C. Gaona Tiburcio<sup>1</sup>, O. Samaniego-Gómez<sup>1</sup>, J.M. Jáquez-Muñoz<sup>1,2\*</sup>, M.A. Baltazar-Zamora<sup>2</sup>, L. Landa-Ruiz<sup>2</sup>, A. Lira-Martínez<sup>3</sup>, J.P. Flores-De los Ríos<sup>4</sup>, J. Cabral-Miramontes<sup>1</sup>, F. Estupinán-López<sup>1</sup>, F. Almeraya-Calderon<sup>1\*</sup>

<sup>1</sup> Universidad Autónoma de Nuevo León, Facultad de Ingeniería Mecánica y Eléctrica, Centro de Investigación e Innovación en Ingeniería Aeronáutica (CIIIA), Av. Universidad s/n, Ciudad Universitaria, San Nicolás de los Garza, Nuevo León 66455, México

<sup>2</sup> Facultad de Ingeniería Civil-Xalapa, Universidad Veracruzana, Lomas del Estadio S/N, Zona Universitaria, 91000 Xalapa, Veracruz, Mexico

<sup>3</sup> Universidad Autónoma de Ciudad Juárez, Instituto de Ingeniería y Tecnología (IIT), Av. Del Charro 150 N, Ciudad Juárez Chihuahua 32584, Mexico.

<sup>4</sup> Department Metal-Mechanical, Tecnológico Nacional de Mexico-Instituto Tecnológico de Chihuahua, Av. Tecnológico 2909, Chihuahua 31130, Mexico

\*E-mail: [jesus.jaquezmn@uanl.edu.mx](mailto:jesus.jaquezmn@uanl.edu.mx); [facundo.almerayacl@uanl.edu.mx](mailto:facundo.almerayacl@uanl.edu.mx)

Received: 2 June 2022 / Accepted: 19 July 2022 / Published: 7 August 2022

---

Precipitation-hardening stainless steel is frequently utilized in a variety of aerospace applications. While the latter steel is employed in applications demanding great strength and corrosion resistance, the former steel offers good corrosion resistance with moderate strength. In this work, the corrosion behavior of AM 350 stainless steel exposed to solutions containing 5% NaCl and 1% H<sub>2</sub>SO<sub>4</sub> after being passivated in nitric acid and citric acid solution for 50 min each at 49 and 70°C is examined. AM 350 stainless steel is precipitation hardening stainless steel, widely used in various aerospace applications. The former steel exhibits excellent corrosion resistance with moderate strength, whereas the latter is used for applications requiring high strength and corrosion resistance. In this study, AM 350 stainless steel corrosion behavior passivated in a) citric acid and b) nitric acid solutions for 50 min at 49 and 70 °C, and subsequently exposed in 5 wt. % NaCl and 1 wt. % H<sub>2</sub>SO<sub>4</sub> solutions are investigated. The electrochemical technique used was electrochemical noise (EN), based on the ASTM G199 standards. Two data analysis techniques were employed for EN: the time-frequency domain (wavelets transform) and the power spectral density (PSD). The results showed a better behavior against corrosion of samples passivated in nitric acid in citric acid. Also, in NaCl electrolyte, the uniform process is the predominant behavior.

---

**Keywords:** stainless steel, electrochemical noise, passivation, FFT, Wavelets.

## 1. INTRODUCTION

One of the biggest problems in the aeronautic industry is the corrosion of aircraft components, increasing costs, and decreasing safety. Nowadays, the methods to protect materials against corrosion seek to decrease the environmental impact by reducing the contamination of some processes as passivation. The passivation is one of the most common methods used in stainless steels (SS), increasing the resistance of steel against corrosion [1-4].

The classification of stainless steels can be divided according to the microstructure, austenitic ( $\gamma$ ), ferritic ( $\alpha$ ), duplex ( $\alpha+\gamma$ ), precipitation hardening (PH), and martensitic ( $\gamma'$ ) [1, 5-6]. Due to the good performance in critical conditions, the aeronautical industry employs PH, martensitic, and austenitic in actuators, landing gear supports, and fasteners [6, 8].

The PH stainless steels (PHSS) have excellent corrosion resistance, and heat treatment can be applied to change mechanical and corrosion properties. The PHSS are divided into semi-austenitic, austenitic, and martensitic [9-16].

Several types of research on SS are focused on calculated corrosion rates, pitting potentials, corrosion mechanisms, and passive-transpassive regions of passivation samples employing potentiodynamic polarization (PP), electrochemical impedance spectroscopy (EIS), galvanodynamic polarization (GP), and electrochemical noise (EN) techniques [17-20].

The advantages of working with the electrochemical noise technique are that it is a non-perturbative test and describes the electrochemical processes that occur when current or potential change can be fluctuations or transients [21-23]. The transients can explain different reactions, such as cathodic or anodic, related to the passive film's rupture and regeneration. Also, continuous transients can be related to pitting formation and propagation [25-26]. Another EN advantage is that it provides valuable information about the process of localized corrosion.

Factors such as the working electrodes' surface area, electrode symmetry, and electrolyte resistance directly influence EN measurement. Diverses authors suggested different methods to study EN data. The methods are divided into frequency domain, time-domain, and time-frequency domain. The time-domain methods are more common to study and consist of analyses of statistical parameters such as skewness, Kurtosis, noise resistance, localization index (LI), and standard deviation; those analyses are the most reported. The frequency-domain analysis consists of transform signals as FFT (fast Fourier transforms) for PSD (power spectral density), shot noise, and noise impedance. Finally, time-frequency-domains study the HHT (Hilbert-Huang transform), Stockwell transform, DWT (discrete wavelet transform), Shannon entropy, etc [27-30].

Suresh and Mudali [31] investigated the AISI 304 SS by applying EN determining localized corrosion when AISI 304 is in  $\text{FeCl}_3$ . Lara et al. [32] characterized PHSS (15-5 and 17-4) by EN and PPC techniques obtaining that the oxide layer generated in both media is similar. Bragaglia et al. [33] employed PP in 304 AISI SS with passivation and uncoated. The results showed an increase in pitting potential for passivated samples related to using nitric acid as a passivation electrolyte. Marcelin et al. [34] studied that a passive layer was formed by air exposition. And other authors characterized the electrochemical behavior of PHSS by employing EIS and EN [35]. The results showed that CUSTOM 450 PHSS has better properties against corrosion. Elements such as chromium increase the corrosion

resistance in PHSS by generating a Cr<sub>2</sub>O<sub>3</sub> layer [36-37]. One way to obtain this oxide layer is by passivation, based on ASTM A967 [22].

This work aims to characterize the AM350 PHSS in nitric and citric acid passivation electrolytes at 49 and 70°C at different exposure times (50 min) in 5 wt. % NaCl and 1 wt. % H<sub>2</sub>SO<sub>4</sub> solutions uses electrochemical noise (EN) technique.

## 2. MATERIALS AND METHODS

### 2.1. Materials

The material used in this work was AM350 (UNS35000) stainless steel. The nominal chemical composition of this stainless steel [35] is shown in Table 1.

**Table 1.** Chemical composition of the AM350 SS (wt. %).

<i>Alloy</i>	<i>Fe</i>	<i>Cr</i>	<i>Ni</i>	<i>Mo</i>	<i>Mn</i>	<i>Cu</i>	<i>Ti</i>	<i>Nb</i>	<i>N</i>	<i>Si</i>	<i>C</i>	<i>S</i>
<b>AM350</b>	Balance	16.0– 17.0	4.0– 5.0	2.50– 3.25	0.50– 1.25	–	–	–	0.07– 0.13	≤0.50	0.07– 0.11	0.030

### 2.2 Passivation Treatment

The passivation was made it followed the ASTM A9677-17 and ASTM A380-17 specifications regulating the pretreatment [degreased and pickling in a 50 wt.% HCl for 5 s at 25 °C and rinsed in distilled water], Passivation treatment [passivation baths, passivation time and temperature], and final treatment [Rinsed in distilled water] [22, 37]. A DoE 5 (design of experiments) was employed due to the acid combinations, concentration, temperature, and passivation time, See Figure 1. Table 2 shows the parameters of passivation treatment for each type of PHSS.

**Table 2.** Nomenclature and passivation treatment parameters.

PHSS	Nomenclature samples *	Passivation Baths	Time (min)	Temperature (°C)
AM 350	CA-50min-49 °C	Citric acid - C <sub>6</sub> H <sub>8</sub> O <sub>7</sub>	50	49
	NA-50min-70 °C	Nitric acid - HNO <sub>3</sub>		70
	NA-50min-70 °C	Nitric acid - HNO <sub>3</sub>		70
	CA-50min-49 °C	Citric acid - C <sub>6</sub> H <sub>8</sub> O <sub>7</sub>		49

\* Citric acid (CA) and Nitric acid (NA)

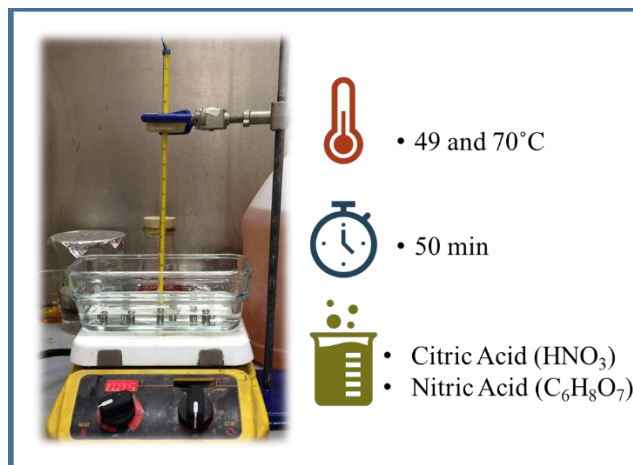


**Figure 1.** Diagram of passivation treatment of AM 350 PHSS. Two passivation baths of nitric acid (20% v) and citric acid (55% v) solutions were used. A constant temperature of 49 and 70 °C was maintained through the passivation treatment. Specimens were immersed in the solutions for 50 min.

### 2.3. Microstructural Characterization

AM 350 samples were prepared by metallography technique. The grinding was made with SiC sandpaper (from 400 to 800 grade) to be cleaned for 10 minutes in ultrasonic with ethanol and deionized water [38].

The microstructure was determined by optical microscopy (OM) and scanning electron microscopy (SEM, JEOL-JSM-5610) with secondary electrons (SE) at 500× and 2000×.

### 2.4. Electrochemical Test

#### 2.4.1. Electrochemical Noise

The EN characterization was made of 1024 data, 1 data per second. The cell array consisted of three electrodes, the working electrode (AM350), the reference electrode (SCE), and a platinum wire of the working electrode 2. The data were filtered with the polynomial method (9°). Power Spectral Density, polynomial filter, and wavelet transformed were applied using a MATLAB 2018a program. All measurements were based on ASTM G199-09 and triplicate [39-41].

##### 2.4.1.1. Polynomial Method

The trend signal (DC) separation is necessary to eliminate interference signals for the different EN analysis methods. To obtain a filtered signal ( $y_n$ ) is necessary to apply a polynomial ( $p_o$ ) of grade “n” at n-th term ( $a_i$ ) [42].

$$y_n = x_n - \sum_{i=0}^{p_o} a_i n^i \quad (1)$$

2.4.1.2. Power Spectral Density (PSD)

The PSD signal is calculated using the FFT (fast Fourier transform) to a filtered signal, in this case, the current signal.

$$R_{xx}(m) = \frac{1}{N} \sum_{n=0}^{N-m-1} x(n) \cdot x(n+m), \text{ for } m \text{ positive values} \quad (2)$$

$$\Psi_x(k) = \frac{Y \cdot L_m}{N} \cdot \sum_{n=1}^N (x_n - \bar{x}_n) \cdot e^{\frac{-2\pi kn^2}{N}} \quad (3)$$

To interpret PSD is necessary to study the slope specter value, which helps to relate the corrosion type of the system. The following equation calculates the slope ( $\beta_x$ ):

$$\log \Psi_x = -\beta_x \log f \quad (4)$$

Also,  $\psi^0$  (frequency zero limits) can give information about material dissolution when it is analyzed in the current. Table 3 gives the slope values related to different corrosion types [43].

**Table 3.** Intervals of  $\beta$  to determine the corrosion type [43].

Units	Scale	Corrosion type		
		Uniform	Pitting	Passive
dB(A)·decade <sup>-1</sup>	Minimum	0	-7	-1
	Maximum	-7	-14	1

2.4.1.3. Wavelets Method

The wavelets method helps decompose a signal according to the frequency of the process, dividing it into long, middle, and fast processes. The energy (fraction) is divided into crystals. The first and middle crystals are related to the localized process (D1-D6), and the final crystals are related to the controlled, diffusion, or generalized process due to a long-time duration [44-47].

$$E = \sum_{n=1}^N x_n^2 \quad (5)$$

$$ED_j^d = \frac{1}{E} \sum_{n=1}^N d_{j,n}^2 \quad ED_j^s = \frac{1}{E} \sum_{n=1}^N s_{j,n}^2 \quad (6)$$

$$E = ED_j^s \sum_{j=1}^j ED_j^d \quad (7)$$

Table 4 shows the crystals' range scale in seconds and Hz [44].

**Table 4.** Ranges of crystals scale

Crystal (D)	Scale (s)	Scale (Hz)
1	1 - 2	1 - 0.5
2	2 - 4	0.5 - 0.25
3	4 - 8	0.25 - 0.125
4	8 -16	0.125 - 0.0625
5	16 - 32	0.0625 - 0.3125
6	32 - 64	0.03125 - 0.015625
7	64 - 128	0.015625 - 0.00781
8	128 - 256	0.00781 - 0.00390

### 3. RESULTS AND DISCUSSION

#### 3.1. OM-SEM microstructural

Figure 2 shows the microstructures obtained by OM and SEM-SE analysis. Figure 2a shows the microstructure by OM; the austenitic phase is present in microstructure of AM350 with the delta ( $\delta$ ) ferrite phase. In figure 2b, the microstructure by SEM corroborates the results. [49-50].

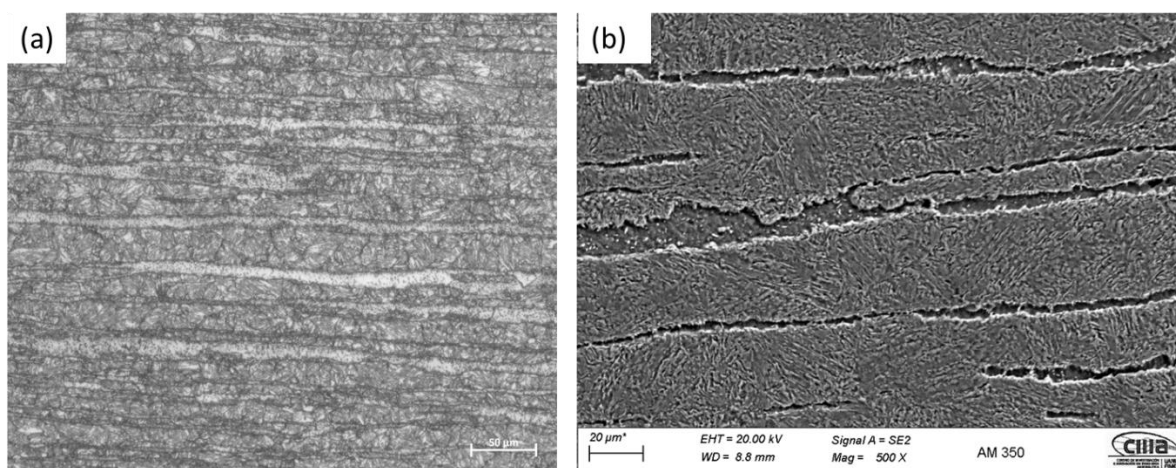


**Figure 2.** Microstructure of AM 350 precipitation hardening stainless steel (initial conditions): (a) Optical microscopy (OM) and (b) scanning electron microscopy with secondary electrons SEM-SE

The pitting resistance equivalent number (PREN) is related with pitting corrosion and helps to compare different SS pitting tendencies [51-53]. If PREN is high is related to high resistance against pitting corrosion. PREN can be determined with the following equation:

$$PREN = Cr + 3.3Mo + 16N \quad (8)$$

**Table 5.** Pitting resistance equivalent number (PREN) analysis of AM350.

<i>PHSS</i>	<i>Cr</i>	<i>Mo</i>	<i>N</i>	<i>PREN</i>
<b>AM350</b>	16.0–17.0	2.50–3.25	0.07–0.13	25.37

### 3.1. Electrochemical measurements

#### 3.1.1. Electrochemical Noise

Figure 3a and 4a shows the time series of passivate steels exposed to NaCl electrolyte. The electrochemical potential noise (EPN) is presented in figure 3a. All the samples showed a decrease in voltage amplitude in time function. The reduction of amplitude is related to the stabilization of ionic exchange. The sample NA-50min-70°C presented amplitudes of  $3 \times 10^{-2}$  V, the higher demand. Also, the electrochemical current noise (ECN) from figure 4a showed that sample NA-50min-70°C has a higher current amplitude ( $3 \times 10^{-6}$  A·cm<sup>-2</sup>). This behavior is related to increase in corrosion kinetic. The sample CA-50min-49°C showed a similar behavior but amplitudes of  $1 \times 10^{-6}$  A·cm<sup>-2</sup>, meaning that resistance to charge transference is higher. However, as time passes, the sample passivated in nitric acid reduces the current demand, reducing ion and charge transference due to a more stable passive layer. The relation between the current and potential is necessary to obtain corrosion resistance [54-55].

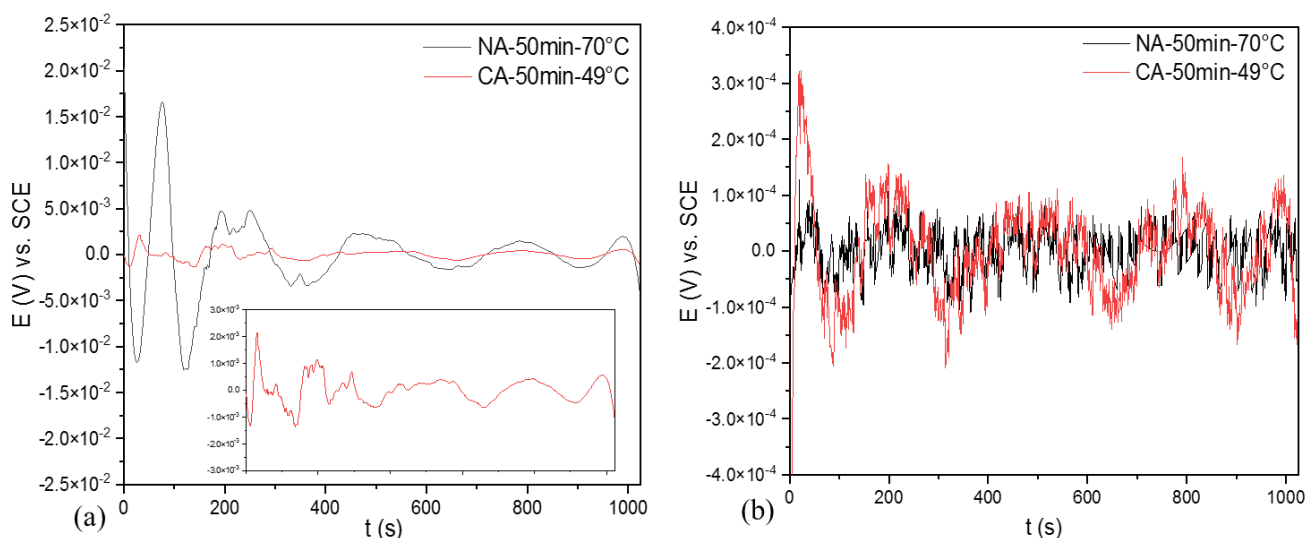


**Figure 3.** Electrochemical potential noise (EPN), for AM350 passivated stainless steels immersed in (a) 5 wt. % NaCl and (b) 1 wt. % H<sub>2</sub>SO<sub>4</sub> solutions.

The EPN series of figure 3b shows the behavior of passivate steels exposed in H<sub>2</sub>SO<sub>4</sub>. Both samples presented low amplitudes ( $2 \times 10^{-4}$  V). The low fluctuation can be related to the generation of the passive layer. In ECN of figure 4b, the samples presented transients. However, the transients were

of low amplitude for NA-50min-70°C ( $3 \times 10^{-7} \text{ A} \cdot \text{cm}^{-2}$ ), while for CA-50min-49°C, the transients were of  $1.4 \times 10^{-6} \text{ A} \cdot \text{cm}^{-2}$ . This behavior can be related to localized corrosion due to breaking and regenerating the passive layer or breaking and pitting of material.

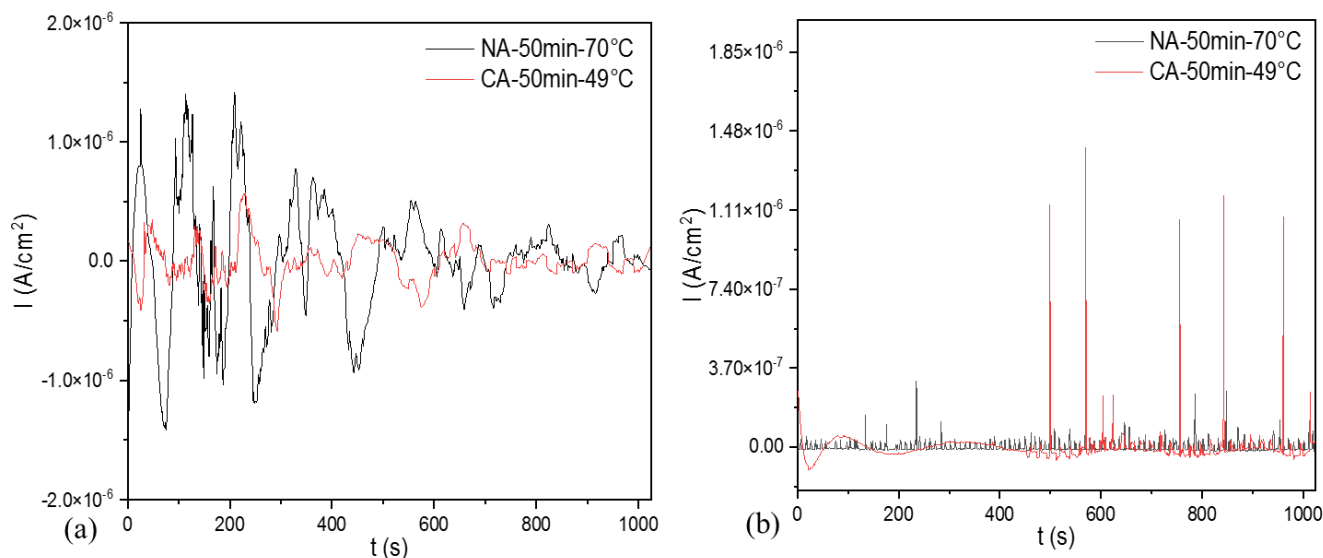


**Figure 4.** Electrochemical current noise (ECN)–time series, for AM 350 passivated stainless steels immersed in (a) 5 wt. % NaCl and (b) 1 wt. % H<sub>2</sub>SO<sub>4</sub> solutions.

3.1.1.1. Statistical Analysis

The statistical analysis shows that samples in NaCl presented uniform corrosion. When passivated samples were exposed to H<sub>2</sub>SO<sub>4</sub> presented localized and mixed corrosion. The results obtained by skewness corroborated the LI results in both electrolytes (see table 6). It is essential to mention that samples anodized in nitric acid presented a higher noise resistance, meaning a higher resistance against corrosion. [56-57]

**Table 6.** Electrochemical noise statistical parameters from passivated AM 350 stainless steels immersed in 5 wt. % NaCl and 1 wt. % H<sub>2</sub>SO<sub>4</sub> solutions.

Solutions	Samples	Noise Resistance $R_n$ (ohm)	Location Index LI	Type of Corrosion	Skewness	Type of Corrosion
Sodium Chloride (NaCl)	NA-50min-70 °C	873.0	0.009	Uni	-0.23	Uni
	CA-50min-49 °C	3047.0	0.003	Uni	0.14	Uni
Sulfuric Acid (H <sub>2</sub> SO <sub>4</sub> )	NA-50min-70 °C	1571.0	0.20	Loc	1.70	Loc
	CA-50min-49 °C	1055.0	0.04	Mix	2.40	Loc

### 3.1.1.2 Power Spectral Density Analysis and Noise Impedance ( $Z_n$ )

Figure 5a shows the PSD of the ECN signal. Both samples present a similar  $\Psi^0$  value ( $-129$  dBi). Also, the behavior of slope in all frequencies is very similar,  $-12$  and  $-14$ , related to a pitting corrosion process. In figure 6a, the value of  $Z_{n0}$  of NA-50min-70°C is  $75386 \Omega \cdot \text{cm}^2$ , and of CA-50min-49°C is  $25491 \Omega \cdot \text{cm}^2$ , meaning a higher corrosion resistance for sample anodized in nitric acid. [55, 58-59]

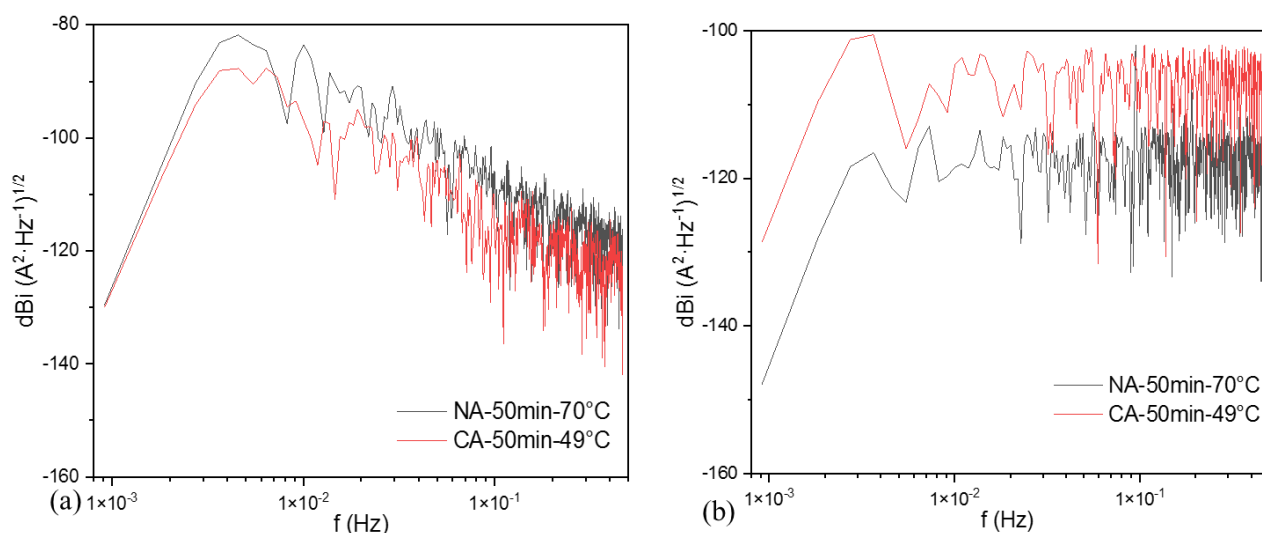


**Figure 5.** Power spectral density (PSD) for AM 350 passivated stainless steels immersed in (a) 5 wt. % NaCl and (b) 1 wt. %  $\text{H}_2\text{SO}_4$  solutions.

Figure 5b shows the PSD of ECN in  $\text{H}_2\text{SO}_4$ . In this case, the sample anodized in citric acid presented a higher value of  $\Psi^0$  and in figure 6b the lower  $Z_{n0}$  ( $-128$  dBi and  $3832 \Omega \cdot \text{cm}^2$ ), meaning that corrosion kinetic is higher than anodized with nitric acid. However, both samples presented slope values related to uniform corrosion. However, some changes in slope at high frequencies can be related to an unstable passive layer. The results obtained by this method are related to a passive layer development and the regeneration of this one.

The results obtained by  $Z_{n0}$  correspond to the noise resistance ( $R_n$ ) from tables 6 and 7, respectively, indicating a close relation between noise impedance and noise resistance from the frequency and time domain. Diverse authors [60-62] associated the two resistances with homologous with  $R_p$ , but with the EN technique.

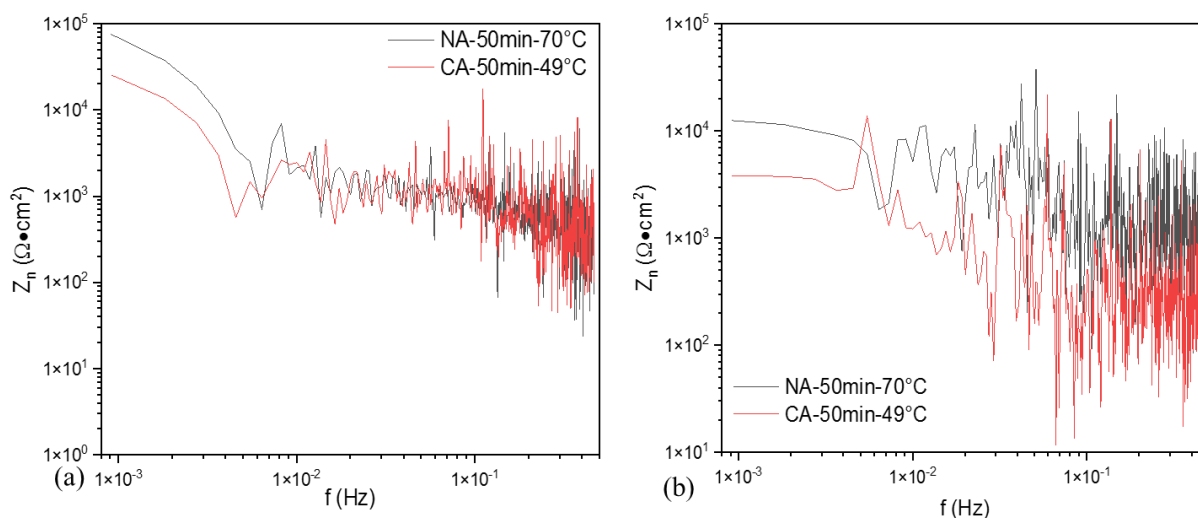


**Figure 6.** Noise impedance ( $Z_n$ ) for AM 350 passivated stainless steels immersed in 5 wt. % NaCl and 1 wt. %  $H_2SO_4$  solutions.

Table 7 shows the PSD parameters. Pitting corrosion in NaCl electrolyte can be related to the  $Cl^-$  ions that attack the passivated surface. However, the values obtained by slope values differed from those obtained by statistical analysis. For this reason, another analysis method must be employed to corroborate the type of corrosion occurring on the surface. Almeraya et al. [55] mentioned that this class of passivate presented higher corrosion rates when were exposed in sulfuric acid. This behavior can be related with the  $OH^-$  reaction on passivate surface, dissolving easier the passivate and also part of PHSS.

**Table 7.** Parameters obtained by Power Spectral Density Analysis and Noise Impedance ( $Z_n$ ).

Solutions	Samples	Slope B (dB (A))	Noise impedance $Z_{n0}$ ( $\Omega \cdot cm^2$ )	Type of Corrosion	Frequency Zero $\Psi^0$ (dBi)
Sodium Chloride (NaCl)	AM350-NA-50min-70°C	-14	75386	Loc	-129.557
	AM350-CA-50min-49°C	-12	25491	Loc	-129.978
Sulfuric Acid ( $H_2SO_4$ )	AM350-NA-50min-70°C	2	12574	Uni	-147.885
	AM350-CA-50min-49°C	1	3832	Uni	-128.661

### 3.1.1.3. Wavelets Analysis

Figure 7 shows the EDP (energy dispersion plot) of AM350 passivate in passivation samples. When samples were exposed to NaCl (figure 7a), both samples presented a higher energy accumulation in crystals D7 and D8. Those crystals are associated with a process of long duration as uniform corrosion of diffusion (species or pitting). On the other hand, when samples are exposed to  $H_2SO_4$  (figure 7b), the

steel passivated in nitric acid presented high accumulation of in crystals the first three and D8. This behavior is associated to a possible pitting diffusion due to an unstable passive layer. The steel passivated in citric acid presented a higher energy accumulation in the last crystals (D7 and D8), related the process with uniform corrosion [3, 63-64].

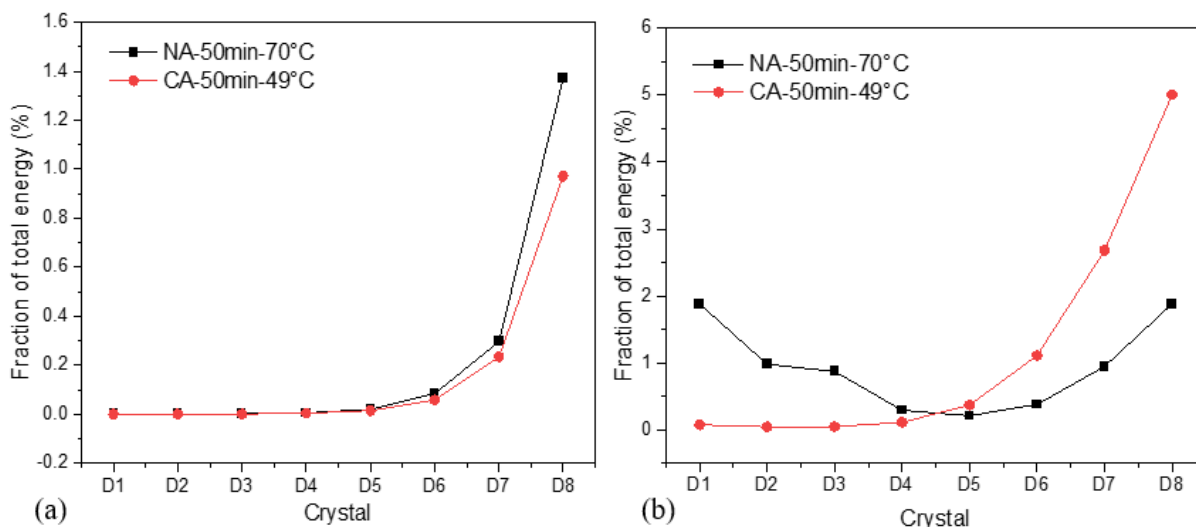


**Figure 7.** Energy Dispersion Plot (EDP) calculated by wavelets method for AM 350 passivated stainless steels immersed in (a) 5 wt. % NaCl and (b) 1 wt. % H<sub>2</sub>SO<sub>4</sub> solutions.

### 3.2. SEM microstructural analysis

Figure 8 shows the SEM analysis of samples after the EN test. Figure 8 a-b shows the damage caused by NaCl. Both samples presented the pitting process, but the pitting was distributed uniformly, related to a pitting diffusion on the surface. Also, pitting is in micrometers' order.

The results matched with the EDP from figure 7a, where a long-time process (diffusion) is present in both samples. Figure 8 c-d show the damage caused by H<sub>2</sub>SO<sub>4</sub>. Figure 8c shows one significant pitting surrounded by minor pitting. This behavior can be associated with pitting nucleation in figure 6b, where NA-50min-70°C presented high energy in the first crystals. However, the minor pitting around the biggest meaning is the begging of a diffusion process. For that reason, figure 7b showed a high energy accumulation in D7 and D8 crystals for NA-50min-70°C, so pitting diffusion is slower for this sample. The behavior presented for passivated in citric acid is of pitting diffusion around the biggest pitting. [3, 44, 65]

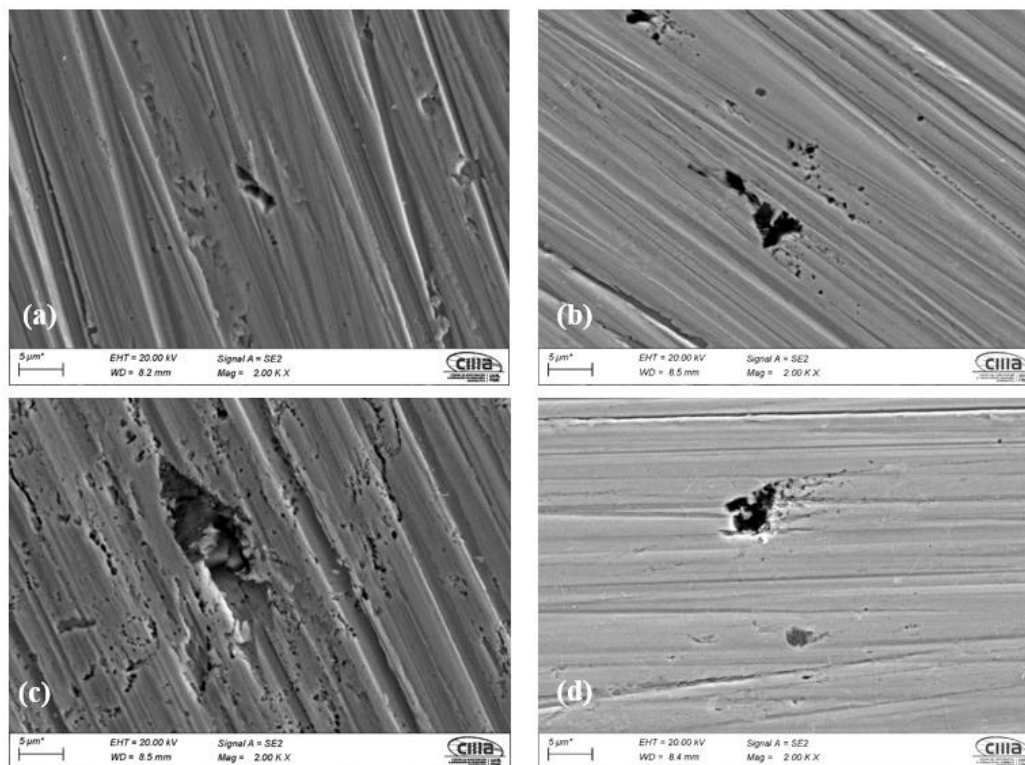


**Figure 8.** SEM-SE analysis of AM 350 PHSS immersed in 5 wt. % NaCl solution (a) NA-50min-70°C and (b) CA-50min-49°C. In 1 wt. % H<sub>2</sub>SO<sub>4</sub> solution (c) NA-50min-70°C and (d) CA-50min-49°C.

#### 4. CONCLUSIONS

- The results indicated that the passivated in citric acid does not generate a better passive layer than in nitric acid. This behavior is related to a high presence of chromium oxide in the passive layer because nitric acid can generate chromium oxide more easily than citric acid. However, those results do not mean that citric acid is a bad option to passivate samples, but in AM350, PHSS is not better than nitric acid passivation.
- For the passivate samples, statistical and wavelets analysis presented a better option to determine the surface corrosion type.
- Also, statistical analysis can be a good option to study passivate SS in electrochemical noise.
- The results in the time-frequency domain indicate that the alloy passivate in nitric acid exposed in H<sub>2</sub>SO<sub>4</sub> presented high energy accumulation in the first crystals; this behavior can be related to a localized process propitious by nitric acid passivation.
- The values of noise resistance ( $R_n$ ) and noise impedance ( $Z_n0$ ) can be cataloged as homologous due to their similar behavior, reflecting the relation with corrosion rate.
- The aggressive H<sub>2</sub>SO<sub>4</sub> is related to the lower corrosion resistance values. Also, it means that the passive layer can be diluted in the electrolyte; also, the anodized in citric acid can

be diluted easier than in nitric acid.

- SEM postmortem analysis corroborates the results of the wavelets and statistical methods. Also, the SEM figure shows a predominance of pitting diffusion and nucleation on the surface of passivating samples.

## ACKNOWLEDGMENTS

The authors thank the Mexican National Council for Science and Technology (CONACYT) for supporting the projects A1-S-8882, the UANL-CA-316 working group, and Universidad Autónoma de Nuevo León (UANL) for the facilities given to developing this investigation and the technical assistance from M. Sc. Luis G. Silva Vidaurri.

## References

1. B. Su, B. Wang, L. Luo, L. Wang, Y. Su, Y. Xu, B. Li, T. Li, H. Huang, J. Guo, H. Fu, and Y. Zou, *Mater. Des.*, 214 (2022) 110416.
2. P. Bocchetta, L.-Y. Chen, J. D. C. Tardelli, A. C. dos Reis, F. Almeraya-Calderón, and P. Leo, *Coatings.*, 11 (2021) 487.
3. J.M. Jaquez-Muñoz, C. Gaona-Tiburcio, A. Lira-Martinez, P. Zambrano-Robledo, E. Maldonado-Bandala, O. Samaniego-Gamez, D. Nieves-Mendoza, J. Olguin-Coca, F. Estupiñan-Lopez and F. Almeraya-Calderon. *Metals.*, 11 (2021) 1002
4. P. Fernandes Santos, M. Niinomi, H. Liu, K. Cho, M. Nakai, A. Trenggono, S. Champagne, H. Hermawan and T. Narushima, *Mater. Des.*, 110 (2016) 414.
5. D.Q. Martins, W.R. Osório, M.E.P. Souza, R. Caram and A. Garcia, *Electrochim. Acta.*, 53 (2008) 2809.
6. B. Su, B. Wang, L. Luo, L. Wang, Y. Su, Y. Xu, F. Wang, B. Han, H. Huang, J. Guo and H. Fu, *J. Mater. Res. Technol.*, 15 (2021) 4896.
7. L. C. Zhang and L. Y. Chen, *Adv. Eng. Mater.*, 21 (2019) 1801215.
8. H. Y. Kim, Y. Ikehara, J.I. Kim, H. Hosoda, and S. Miyazaki, *Acta Mater.*, 54 (2006) 2419.
9. B. Moretti, V. Pesce, G. Maccagnano, G. Vicenti, P. Lovreglio, L. Soleo and P. Apostoli, *Lancet. Ont.*, 379 (2012) 1676.
10. R. Ion, D. M. Gordin, V. Mitran, P. Osiceanu, S. Dinescu, T. Gloriant and A. Cimpean, *Mater. Sci. Eng. C.*, 35 (2014) 411.
11. M. Chen, L. Yang, L. Zhang, Y. Han, Z. Lu, G. Qin and E. Zhang, *Mater. Sci. Eng. C.*, 75 (2017) 906.
12. Z. Liu, X. Liu, U. Donatus, G. E. Thompson and P. Skeldon, *Int. J. Electrochem. Sci.*, 9 (2014) 3558.
13. J.A.Cabral-Miramontes, M.D.Bastidas, M.A.Baltazar, P.Zambrano-Robledo, J.M.Bastidas, F. Almeraya-Calderón, C. Gaona-Tiburcio, *Int. J. Electrochem. Sci.*, 14 (2019) 4226.
14. D. F. Ferreira, S. M. A. Almeida, R. B. Soares, L. Juliani, A. Q. Bracarense, V. D. F. C. Lins, and R. M. R. Junqueira, *J. Mater. Res. Technol.*, 8 (2019) 1593.
15. S. Noumbissi, A. Scarano and S. Gupta, *Materials.*, 12 (2019) 368.
16. S. Attabi, M. Mokhtari, Y. Taibi, I. Abdel-Rahman, B. Hafez and H. Elmsellem, *J. Bio- Tribo- Corros.*, 5 (2018) 1.
17. D. H. Xia, S. Z. Song and Y. Behnamian, *Electrochim. Acta.*, 51 (2016) 527.
18. C. Liu, A. Leyland, Q. Bi and A. Matthews, *Surf. Coatings Technol.*, 141 (2001) 164.
19. R.E. Núñez-Jaquez, J.E. Buelna-Rodríguez, C.P. Barrios-Durstewitz, C. Gaona-Tiburcio and F.

- Almeraya-Calderón, *Int. J. Corros.*, 52 (2012) 451864.
20. N.T.C. Oliveira and A. C. Guastaldi, *Acta Biomater.*, 5 (2009) 399.
  21. X.Q. Du, Q.S. Yang, Y. Chen, Y. Yang and Z. Zhang, *Trans. Nonferrous Met. Soc. China.*, 24 (2014) 570.
  22. ASTM A967-17; Standard Specification for Chemical Passivation Treatments for Stainless Steel Parts. ASTM International: West Conshohocken, PA, USA (1999).
  23. S. Esmailzadeh, M. Aliofkhaezai and H. Sarlak, *Prot. Met. Phys. Chem. Sur.*, 54 (2018) 976.
  24. T. Shibata, Stochastic studies of passivity breakdown. *Corros. Sci.*, 31 (1990) 413.
  25. F.J. Olguin Coca, M.U. Loya Tello, C. Gaona-Tiburcio, J.A. Romero, A. Martínez-Villafañe, E. Maldonado and F. Almeraya-Calderón, *Int. J. Electrochem. Sci.*, 6 (2011) 3438.
  26. M.J. Pellegrini-Cervantes, F. Almeraya-Calderon, A. Borunda-Terrazas, R.G. Bautista-Margulis, J.G. Chacón-Nava, G. Fajardo-San-Miguel, J.L. Almaral-Sanchez, C. Barrios-Durstewitz and A. Martinez-Villafañe, *Int. J. Electrochem. Sci.*, 8 (2013) 10697–10710.
  27. P. Lewis, M. Kolody, Proceedings of the NASA Technology Evaluation for Environmental Risk Mitigation Principal Center (TEERM); Department of Defense (DoD) and NASA: Kennedy Space Center, Florida, USA, January 13, 2008.
  28. D. Yasensky, J. Reali, C. Larson, C. Carl. In Proceedings of the Aircraft Airworthiness and Sustainment Conference, San Diego, California, USA, 18-21 april, 2009.
  29. U. Bertocci, F. Huet. *Corrosion.*, 51 (1995) 131.
  30. S.P. Gaydos, *Plat. Surf. Finish.*, 90 (2003) 20.
  31. G.U. Suresh, M.S. Kamachi, *Corrosion.*, 70 (2014) 283.
  32. M. Lara-Banda, C. Gaona-Tiburcio, P. Zambrano-Robledo, M. Delgado-E. J. Cabral-Miramontes, D. Nieves-Mendoza, E. Maldonado-Bandala, F. Estupiñan-López, J. Chacón-Nava, F. Almeraya-Calderón, *F. Materials* 13 (2020) 2836,
  33. M. Bragaglia, V. Cherubini, I. Cacciotti, M. Rinaldi, S. Mori, P. Soltani, F. Nanni, S. Kaciulis and G. Montesperelli, In Proceedings of the CEAS Aerospace Europe Conference 2015, Delft, The Netherlands, 7–11 September 2015.
  34. S. Marcelin, N. Pébèrea and S. Régnier, *Electrochim. Acta.*, 87 (2013) 32.
  35. O. Samaniego-Gámez, F. Almeraya-Calderón, J. Chacón-Nava, E. Maldonado-Bandala, D. Nieves-Mendoza, J.P. Flores-De los Rios, J.M. Jáquez-Muñoz,; A.D. Delgado and C. Gaona-Tiburcio. *Metals.*, 12 (2022) 666.
  36. AM 350 Technical Data. Available online: <https://www.hightempmetals.com/techdata/hitempAM350data.php> (accessed on 31 April 2022).
  37. ASTM A380-17; Standard Practice for Cleaning, Descaling and Passivation of Stainless-Steel Parts, Equipment, and Systems. ASTM International: West Conshohocken, PA, USA (1999).
  38. ASTM E3-95. Standard Practice for Preparation of Metallographic Specimens; ASTM International: West Conshohocken, PA, USA (1995).
  39. ASTM G199-09. Standard Guide for Electrochemical Noise Measurement; ASTM International: West Conshohocken, PA, USA (2009).
  40. A. Martínez-Villafañe, F. Almeraya-Calderón, C. Gaona-Tiburcio, J.G. Gonzalez-Rodriguez and Porcayo-Calderón, *J. Mater. Eng. Perform.*, 7 (1998) 108.
  41. J. M. Jáquez-Muñoz, C. Gaona-Tiburcio, J. Cabral-Miramontes, D. Nieves-Mendoza, E. Maldonado-Bandala, J. Olguín-Coca, L. D. López-Léon, J. P. F. De Los Rios and F. Almeraya-Calderón, *Metals.*, 11 (2021) 105.
  42. D.L. Dawson, Kearns, J.R., Scully, J.R., Roberge and P.R., Reirchert, *Eds. STP 1277; ASTM International*, Materials Park: USA (1996) 3.
  43. A. Legat and V. Doleček, *Corrosion.*, 51 (1995) 295.
  44. A.M. Homborg, C.F. Leon Morales, T. Tinga, J.H.W. De Wit and J. M. C. Mol, *Electrochim. Acta.*, 136 (2014) 223.
  45. A. Sedriks J. Green and D. Novak, *Corrosion.*, 28 (1972) 137.

46. K. H. W. Seah, R. Thampuran and S. H. Teoh, *Corros. Sci.*, 40 (1998) 547.
47. C. Kuphasuk, Y. Oshida, C. J. Andres, S. T. Hovijitra, M. T. Barco and D. T. Brown, *J. Prosthet. Dent.*, 85 (2001) 195.
48. C. Vasilescu, S. I. Drob, E. I. Neacsu and J. C. Mirza Rosca, *Corros. Sci.*, 65 (2012) 431.
49. J. Dias Corpa Tardelli, C. Bolfarini and A. Cândido dos Reis, *J. Trace Elem. Med. Biol.*, 62 (2020) 126618.
50. A. Gupta, A.K. Bhargava, R. Tewari and A.N. Tiwari. *Metal. Mater. Trans. A* 44 (2013) 4248.
51. X.L. Xu, Z.W. Yu. *J. Mater. Process. Tech.*, 198 (2008) 254.
52. E.E. Maldonado-Bandala, V. Jiménez-Quero, F. Olguin-Coca, M.L.G. Lizarraga, M.A. Baltazar-Zamora, A. Ortiz-C, F. Almeraya, P. Zambrano and C. Gaona-Tiburcio. *Int. J. Electrochem. Sci.*, 6 (2011) 4915.
53. The British Stainless Steel Association 2022. Available online: [https://bssa.org.uk/bssa\\_articles/calculation-of-pren/](https://bssa.org.uk/bssa_articles/calculation-of-pren/) accessed date (accessed on 2 June 2022).
54. P. Schweitzer. *Fundamentals of Metallic Corrosion: Atmospheric and Media Corrosion of Metals*; CRC Press Taylor & Francis Group. 2007, NW, USA.
55. F. Almeraya-Calderón, O. Samaniego-Gámez, E. Maldonado-Bandala, D. Nieves-Mendoza, J. Olguín-Coca, J.M. Jáquez-Muñoz, J. Cabral-Miramontes, J.P. Flores-De los Rios, R.G. Bautista-Margulis and C. Gaona-Tiburcio. *Metals.*, 12 (2022) 1033.
56. C. Monticelli, *J. Electrochem. Soc.*, 139 (1992) 706.
57. C.J. Park and H.S. Kwon, *Mater. Chem. Phys.*, 91 (2005) 355–360.
58. C. Gaona-Tiburcio, F. Almeraya-Calderón, J. Chacon-Nava, A. M. Matutes-Aquino and A. Martinez-Villafañe. *J. Alloys Compd.*, 369 (2004) 78-80.
59. A. Contreras, M. Salazar, A. Carmona, and R. Galván-Martínez, *Mater. Res.*, 20 (2017) 1201.
60. J.M. Jáquez-Muñoz, C. Gaona-Tiburcio, J. Cabral-Miramontes, D. Nieves-Mendoza, E. Maldonado-Bandala, J. Olguín-Coca, F. Estupiñán-López, L.D. López-León, J. Chacón-Nava and F. Almeraya-Caderón. *Metals.*, 11 (2021) 702.
61. A. M. Ramirez-Arteaga, J. G. Gonzalez-Rodriguez, B. Campillo, C. Gaona-Tiburcio, G. Dominguez-Patiño, L. Leduc Lezama, J. G. Chacon-Nava, M. A. Neri-Flores, A. Martinez-Villafañe. *Int. J. Electrochem. Sci.*, 5 (2010) 1786.
62. D.A. Eden, *Corrosion/98 NACE.*, 30 (1998) 1-31.
63. J. Li, C.W. Du, Z.Y. Liu, X.G. Li and M. Liu, *Const. and Build. Mater.*, 189 (2018) 1294.
64. G. Santiago-Hurtado, M.A. Baltazar-Zamora, R. Galván-Martínez, L. D. López L, F. Zapata G, P-Zambrano, C. Gaona-Tiburcio and F. Almeraya-Calderón. *Int. J. Electrochem. Sci.*, 11 (2016) 4850.
65. J. Cui, D. Yu, Z. Long, B. Xi, X. He and Y. Pei. *J. Electroanal. Chem.*, 855 (2019) 113584.